Applied Catalysis B: Environmental 111–112 (2012) 628–635

Contents lists available at SciVerse ScienceDirect

Applied Catalysis B: Environmental

journal homepage: www.elsevier.com/locate/apcatb

The electrocatalytic dechlorination of chloroacetic acids at electrodeposited Pd/Fe-modified carbon paper electrode

Angzhen Li[a,b], Xu Zhao[a], Yining Hou[a], Huijuan Liu[a], Liyuan Wu[a], Jiuhui Qu[a,*]

[a] State Key Laboratory of Environmental Aquatic Chemistry, Research Center for Eco-Environmental Sciences, Chinese Academy of Sciences, Beijing 100085, China
[b] Graduate School, Chinese Academy of Sciences, Beijing 100039, China

ARTICLE INFO

Article history:
Received 11 August 2011
Received in revised form 5 November 2011
Accepted 7 November 2011
Available online 18 November 2011

Keywords:
Pd/Fe-modified carbon paper electrode
Electrocatalytic dechlorination
Chloroacetic acids
Direct reduction
Indirect reduction

ABSTRACT

Pd/Fe-modified carbon paper (Pd/Fe-C) electrode was prepared from $PdCl_2$ and $FeSO_4$ via electrodeposition onto carbon paper. It was observed that the diameters of electrodeposited Pd/Fe particles were around 20 nm with a uniform distribution on carbon paper, which is smaller than Pd/Fe particles of impregnated and calcined electrode. The electrodeposited Pd/Fe-C electrode exhibited higher activity in dechlorination of chloroacetic acids than impregnated and calcined electrode. Under optimal experiment conditions of Pd:Fe molar ratio of 2:1 at −1.5 V (vs SCE), 95% of trichloroacetic acid (TCAA) with the initial concentration of 500 μg/L was removed within 20 min at pH 3. The dechlorination of chloroacetic acids followed the order of TCAA > dichloroacetic acid (DCAA) > monochloroacetic acid (MCAA). MCAA cannot be dechlorinated at C and Fe-C electrodes via direct reduction. However, a part of chloroacetic acids was directly dechlorinated to acetic acid at Pd-C and Pd/Fe-C electrodes via indirect reduction. The Pd(0) and Pd(II) species were detected by X-ray photoelectron spectroscopy. Compared with the individual Pd-C electrode, in situ formation of Fe(0) decreased the interface impedance as observed by electrochemical impedance spectroscopy analysis. In conclusion, the presence of Pd(0) nanoparticles played a significant role in forming atomic H* to realize indirect reduction process which could achieve the complete dechlorination of chloroacetic acids.

1. Introduction

Chloroacetic acids, including trichloroacetic acid (TCAA), dichloroacetic acid (DCAA), and monochloroacetic acid (MCAA) are ubiquitous in chlorinated water as disinfection byproducts (DBPs). Chloroacetic acids are proved to be carcinogenic and potentially of great risk to human health [1,2]. Conventional decontamination techniques such as adsorption by granular activated carbon or air stripping perform poorly for chloroacetic acids removal due to their high hydrophilicity and stability [3,4]. Though some bacteria could aerobically degrade chloroacetic acids, biodegradation may cause bacterial contamination in water [5,6]. Application of TiO_2 photocatalysis has been reported as a promising alternative technology for removal of chloroacetic acids, whereas the problems of TiO_2 separation from aqueous phase are the limitation of photocatalysis treatment [7,8]. Several studies reported the degradation of haloacetic acids with zero-valent iron (ZVI), and their results indicated that MCAA was relatively persistent during reaction with ZVI [9,10].

Electrochemical reductive treatment has been suggested as a promising method for dechlorination of chloroacetic acids. This treatment ensures the selective removal of chlorine atoms from chloroacetic acids without producing toxic byproducts or adding any toxic chemicals [11–13]. Korshin and Jensen reported that copper and gold electrodes showed good activity for haloacetic acids reduction with the exception of MCAA [11]. Altamar et al. found that gold modified electrode revealed high electrocatalytic activity [13]. However, the use of expensive bulk gold is a disadvantage for practical purpose. In recent years, palladium/iron (Pd/Fe) bimetallic catalysts were found to show good catalytic activity and relatively low price for degradation of halogenated organic compounds (HOCs), especially for the dramatic ability to promote C–Cl bond cleavage [14–21]. It was also reported that addition of Fe to low loaded Pd supported on carbon caused an increase of catalytic activity in dechlorination of HOCs compared to Pd-C and they used impregnation and calcination processes to obtain the catalysts [22,23]. However, impregnation and calcinations will lead to large size and poor dispersions of Pd/Fe particles [24]. The catalysts which were acquired by electrodeposition processes exhibited a low catalyst layer thickness (2–10 μm), could prevent sintering in comparison with impregnation and calcination processes, and resulted in a good crystallization and particle formation [25].

* Corresponding author. Tel.: +86 10 62849151; fax: +86 10 62923558.
E-mail addresses: jhqu@rcees.ac.cn, jhqu@mail.rcees.ac.cn (J. Qu).

0926-3373/$ – see front matter © 2011 Elsevier B.V. All rights reserved.
doi:10.1016/j.apcatb.2011.11.016

Furthermore, it was reported that dechlorination of HOCs at cathode surfaces may occur through both direct and indirect mechanisms [15]. Indirect reduction of organic compounds may occur via reaction with atomic H* [16,26]. Wang et al. deduced that H_2 was decomposed into atomic H* by Pd(0) species for chloroacetic acids dechlorination [17]. However, relatively little literature was available on the intermediates and degradation pathway of direct and indirect reductive dechlorination of chloroacetic acids at cathode.

Herein, the Pd/Fe nanoparticles were electrodeposited onto carbon paper and used as a possible candidate cathode for more efficient electrochemical dechlorination of chloroacetic acids. By contrast, Pd/Fe particles were impregnated and calcined onto carbon paper and examined for their electrocatalytic ability. Carbon paper was used as an electrode due to its low cost and good conductivity. Dechlorination efficiency and degradation pathway of chloroacetic acids during the electroreductive process through carbon paper (C), Fe-modified carbon paper (Fe-C), Pd-modified carbon paper (Pd-C) and Pd/Fe-modified carbon paper (Pd/Fe-C) electrodes were compared and studied. The predominant direct and indirect reduction pathways of electrocatalytic chloroacetic acids at Pd/Fe-C electrode were specifically elucidated.

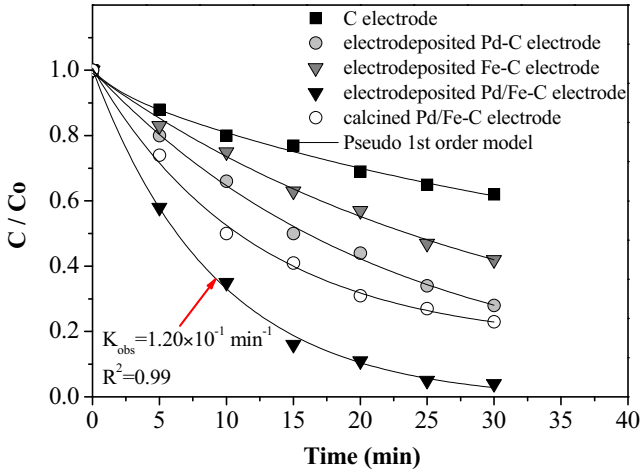

Fig. 1. Dechlorination of TCAA through C, Pd-C, Fe-C and Pd/Fe-C electrodes (initial pH 7.0, Na_2SO_4 = 10 mmol/L, initial TCAA = 500 μg/L, Pd:Fe molar ratio = 2:1, and applied potential = −1.5 V vs SCE).

2. Materials and methods

2.1. Preparation of electrode

The Pd/Fe-C electrode was prepared using the electrodeposition method. The carbon paper was obtained from Beijing LN Power Source Company (Toray 120). Triton X-100 is the highly hydrophobic non-ionic detergent, and the carbon paper was first immersed in a 0.1% (w/w) Triton X-100 (Plusone) solution for 24 h in order to reduce the paper hydrophobicity and form "anchor" sites to lower the extent of metal agglomeration. The wet paper was then immersed in de-ionized water for approximately 2 h [25,27]. The electrodeposition of Pd(0) was carried out by dipping the cleaned carbon paper in dichlorodiamminepalladium [$Pd(NH_3)_2Cl_2$] complex (plating solution), which was formed by 1 mM palladium chloride ($PdCl_2$) and 10 mM ammonium chloride solution [28]. Then, the electrodeposition of Fe(0) was carried out by Pd-modified carbon paper in ferrous sulfate ($FeSO_4{\cdot}7H_2O$) solution. The deposition current and time was 2 mA/cm^2 and 30 min, respectively. The geometric area of the electrodes was 12 cm^2. The electrodeposition process was equipped with an N_2 supply inlet all the while. Also, the Pd/Fe-C electrode was prepared using the impregnation and calcination method. The order and concentration of depositing metal on carbon paper were the same as the electrodeposition method. The material was dried at 105 °C for 12 h and calcined at 300 °C for 120 min under argon. Then, desired amount of second metal (Fe) was loaded from a solution of $FeSO_4{\cdot}7H_2O$ in the same manner. The Pd/Fe-C electrode was acquired by reducing at 200 °C for 120 min under flowing hydrogen. In addition, the Pd/Fe-C electrodes were stored in a N_2-purged desiccator.

2.2. Batch experiment

All electrochemical experiments were carried out in a batch reactor of two-compartment cells with an effective volume of 100 mL. The anode cell (50 mL solution) and cathode cell (50 mL solution) were separated by a cation-exchange membrane (Nafion 117, Dupont). The batch reactor is shown in the Supporting Information (Figure S1). The geometric surface area of cathode was 12 cm^2 (4 cm × 3 cm). Platinum wire, 72 mm in length with a diameter of 1.5 mm, was used as the counter electrode, and a saturated calomel electrode (SCE) was used as the reference electrode. The cathode cell compartment was equipped with an N_2 supply inlet, a gas exit and a sampling port. The power source was an EG&G model 263A workstation (Princeton Applied Research, USA).

2.3. Electrode characterization

Scanning electron microscopy (SEM) and energy-dispersive X-ray spectroscopy (EDX) were carried out in a JSM 6301 instrument. X-ray photoelectron spectroscopy (XPS) analysis was performed with a Kratos AXIS Ultra X-ray photoelectron spectrometer, and Details of XPS were included in the Supporting Information. X-ray powder diffraction (XRD) patterns of samples were obtained with a X'Pert PRO Powder diffractometer machine (PANalytical Co.), by using Ni-filtered Cu K_α radiation from 5° to 90° (in 2θ). Linear scan voltammetry (LSV) analysis was also performed in the EG&G model 263A workstation. Electrochemical impedance spectroscopy (EIS) was recorded in the potentiostatic mode. The amplitude of the sinusoidal wave was 10 mV, and the frequency of the sinusoidal wave was in the range from 0.1 Hz to 100 kHz.

2.4. Analysis method

All solutions were prepared using analytical grade reagents and Milli-Q water (specific conductivity of 18.2 MΩ cm^{-1}). The concentrations of chloroacetic acids and other anions in the effluent from the cathode cell were measured using a Dionex-4500i ion chromatograph (IC) with an IonPac AS-19 anion-exchange analytical column and an IonPac AG19 guard column. Mobile phase eluent for the IC was KOH solution, and the flow rate was 1.0 mL/min. The chromatogram of chloroacetic acids and other anions was obtained under gradient elution conditions (0.0–18.0 min: 10.0 mM KOH; 18.1–30.0 min: 35.0 mM KOH; 30.1–35.0 min: 10.0 mM KOH). The precision of the acetate mass balance in these measurements was ca. 95–105% of the nominal value.

3. Results and discussion

3.1. Dechlorination performance of chloroacetic acids

Firstly, dechlorination of TCAA at electrodeposited Pd-C, Fe-C, Pd/Fe-C electrodes and calcined Pd/Fe-C electrode performed under the same experimental conditions. As shown in Fig. 1, the removal efficiency of TCAA through electrodeposited and calcined Pd/Fe-C cathodes achieved 96% and 77% at 30 min, respectively; meanwhile, the value was 38%, 72% and 58% for C, Pd-C and Fe-C electrodes,

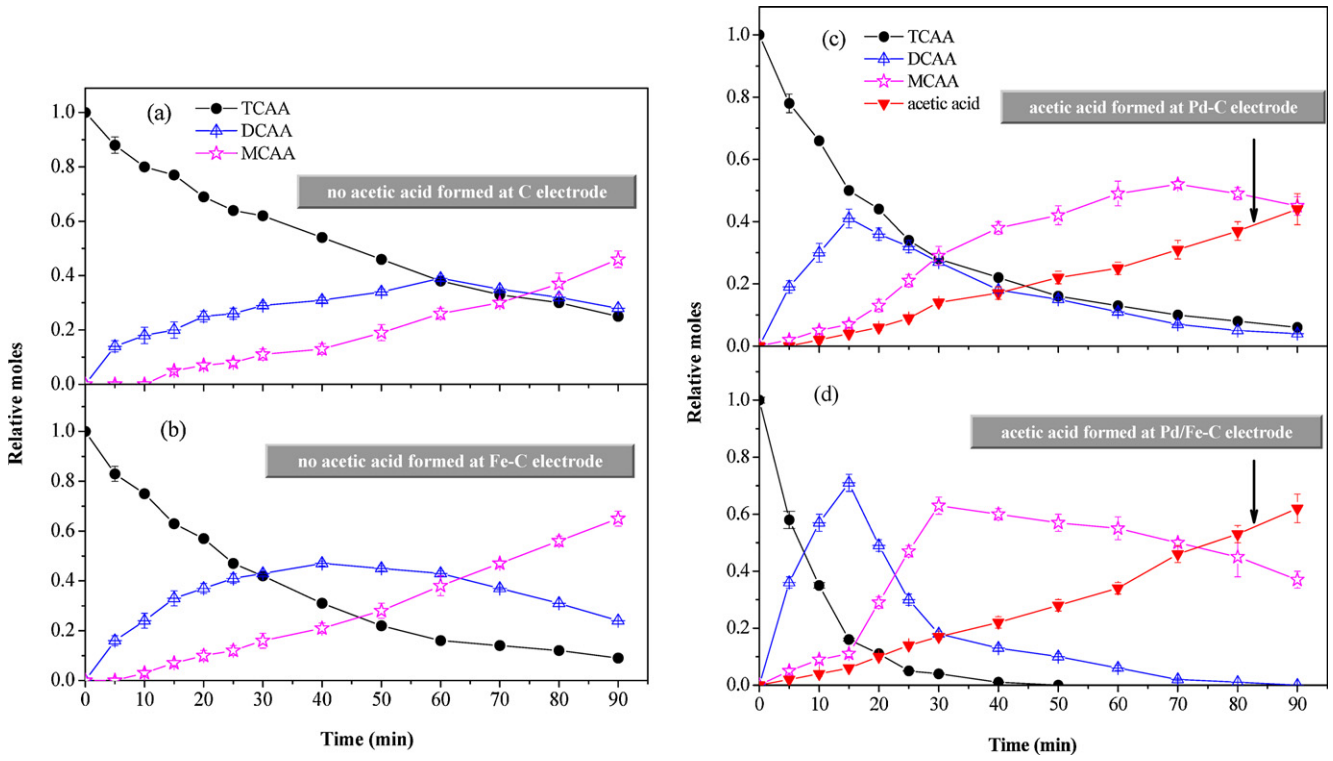

Fig. 2. Intermediates and final products of reductive dechlorination of TCAA through C, Fe-C, Pd-C and Pd/Fe-C electrodes. (a) C electrode; (b) Fe-C electrode; (c) Pd-C electrode; and (d) Pd/Fe-C electrode (initial pH 7.0, Na_2SO_4 = 10 mmol/L, initial TCAA = 500 μg/L, Pd:Fe molar ratio = 2:1, and applied potential = −1.5 V vs SCE).

respectively. Similar removal trends were achieved for MCAA and DCAA (Figure S2). These results indicated that electrodeposited Pd/Fe-C cathode showed much higher electrocatalytic activity in contrast to C, electrodeposited Pd-C, electrodeposited Fe-C, and calcined Pd/Fe-C electrodes for reductive dechlorination.

It was also shown that the dechlorination of chloroacetic acids followed a pseudo-first order kinetic model. The observed reaction rate constants (k_{obs}) of MCAA, DCAA and TCAA through electrodeposited Pd/Fe-C cathode were found to be 3.26×10^{-3} min^{-1} (R^2 = 0.99), 3.87×10^{-2} min^{-1} (R^2 = 0.98) and 1.20×10^{-1} min^{-1} (R^2 = 0.99), respectively. These results demonstrated the electrocatalytic dechlorination rates of chloroacetic acids by Pd/Fe-C electrode followed the order of TCAA > DCAA > MCAA. As atomic chlorine is of high polarity, the number of substituent chlorine would influence the dechlorination efficiency of aliphatic halide, which was consistent with previous research [29,30]. An increased number of chlorines attached to the aliphatic carbon would weaken the C–Cl bond strength [31]. Therefore highly chlorinated chloroacetic acids would be more prone to be dechlorinated during the electrocatalytic process.

The intermediates of the dechlorination of TCAA at C electrode, electrodeposited Fe-C, Pd-C and Pd/Fe-C electrodes are analyzed and illustrated in Fig. 2. TCAA decreased rapidly while DCAA and MCAA as the dechlorination intermediates increased initially, and finally were reduced to acetic acid and chloride ions at Pd-C and Pd/Fe-C cathodes. Meanwhile, the rapid increase in acetic acid concentration revealed the direct conversion of TCAA to acetic acid at Pd-C and Pd/Fe-C cathodes. Stepwise dechlorination of TCAA to MCAA was achieved at C and Fe-C cathodes; however, generated MCAA cannot be dechlorinated. Similar results were also reported by Hozalski et al., who observed that the final product of reactions between chloroacetic acids with Fe(0) was MCAA [9]. Additionally, similar dechlorination pathway was observed for MCAA and DCAA in comparison with TCAA removal (Figures S2–S5). These results indicated that there existed different reduction pathways in the presence of Pd(0) catalysts on carbon paper, which would be analyzed subsequently.

3.2. Effect of Pd:Fe molar ratio on the removal efficiency of chloroacetic acids

According to previously reported results, the Pd:Fe molecular ratio loading on support was an important factor for catalytic activity [14,23]. The molar ratio of Pd:Fe was varied by fixing 1 mM $PdCl_2$ solution and was determined by EDS. The capacity of different Pd:Fe molar ratios for chloroacetic acids dechlorination is compared and presented in Fig. 3. The dechlorination efficiency of chloroacetic

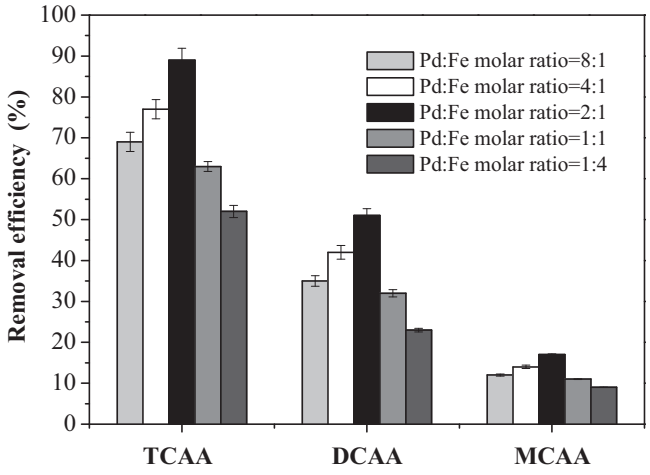

Fig. 3. Effect of Pd:Fe molar ratio on the removal efficiency of chloroacetic acids (initial pH 7.0, Na_2SO_4 = 10 mmol/L, initial concentration of chloroacetic acids = 500 μg/L, reaction time of DCAA and TCAA = 20 min, reaction time of MCAA = 50 min, and applied potential = −1.5 V vs SCE).

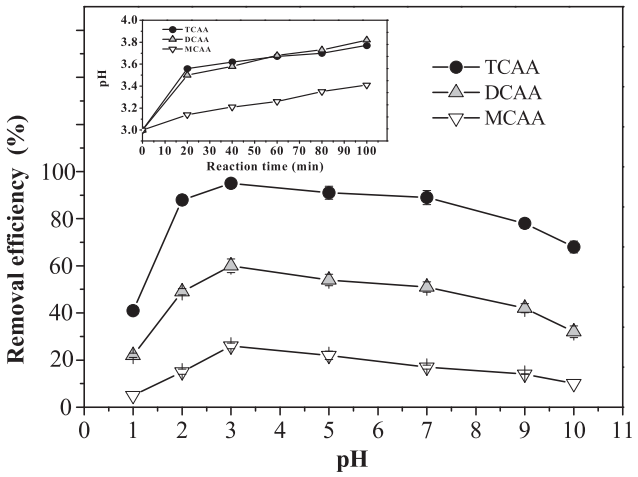

Fig. 4. Effect of initial pH value on the removal efficiency of chloroacetic acids (Na_2SO_4 = 10 mmol/L, initial concentration of chloroacetic acids = 500 μg/L, reaction time of DCAA and TCAA = 20 min, reaction time of MCAA = 50 min, Pd:Fe molar ratio = 2:1, and applied potential = −1.5 V vs SCE).

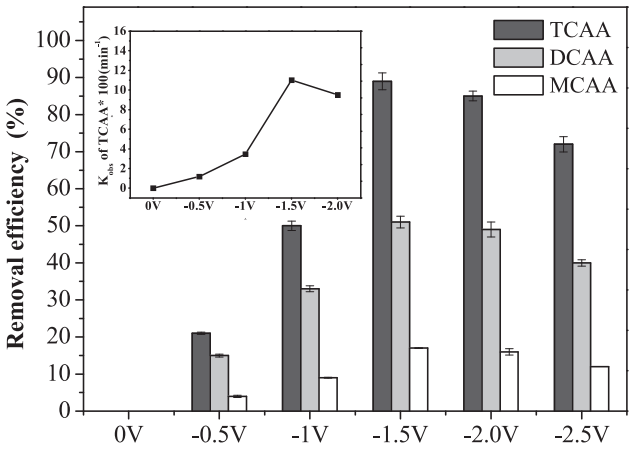

Fig. 5. Effect of applied bias voltage on the removal efficiency of chloroacetic acids (initial pH 7.0, Na_2SO_4 = 10 mmol/L, initial concentration of chloroacetic acids = 500 μg/L, reaction time of DCAA and TCAA = 20 min, reaction time of MCAA = 50 min, and Pd:Fe molar ratio = 2:1).

acids enhanced with increasing the Fe content, with a maximum activity and removal efficiency observed at Pd:Fe molar ratio of 2:1. When the molar ratio of Pd:Fe increased higher than 2:1, a negative influence appeared. For TCAA, the removal efficiency decreased from 89% to 63% as the molar ratio of Pd:Fe increased from 2:1 to 4:1.

This result indicated that the Pd:Fe molar ratio on carbon paper was an important factor for the electrode capacity of chloroacetic acids dechlorination. Golubina et al. [32] reported that atomic ratios of 1:0.5 and 1:2 Pd:Fe offered better activity in the carbon supported catalysts. The presence of Fe(0) nanoparticles played a significant role in modifying the Pd(0) dispersion state and taking up chloride that were liberated during the dechlorination process, thus leaving the Pd(0) component active. Whereas it could be deduced that at high Fe(0) loading the presence of large Fe(0) aggregates on the surface of the catalysts occurred. Then, Fe(0) started covering available Pd(0) (encapsulation) sites, leading to a decrease in the removal efficiency of chloroacetic acids.

3.3. Effect of initial pH value on the removal efficiency of chloroacetic acids

In this experiment, the electrocatalytic dechlorination of chloroacetic acids was performed by changing initial pH values from 1 to 10 in the cathode cell. The initial pH value of the reaction system was adjusted with 0.1 M sodium hydroxide solution and 0.1 M sulfuric acid solution. As illustrated in Fig. 4, the maximum chloroacetic acid removal efficiency occurred at an initial pH of 3.0 in contrast to other values. Additionally, during the dechlorination process pH values increased slightly with the total increase in pH less than 1.

Li and Farrell reported that the reduction of HOCs at Pd plated cathode surfaces may occur through both direct and indirect mechanisms [15]. Indirect reduction of organic compounds may occur via reaction with atomic H* [15,16]. Atomic H* adsorbed on the surface of the electrode at low pH values was beneficial for the reduction of chloroacetic acids. As shown in Fig. 4 inset, the increase of pH value during dechlorination was probably due to the consumption of H*. Whereas an increase in initial pH value of the reaction system could result in OH^- taking up active metals sites and promote the formation of a passive layer due to the precipitation of metal hydroxides on the surface of the electrode. When the solution was under strong acidic conditions, the large amount of hydrogen bubbles adsorbed onto the Pd/Fe interface would inevitably deactivate the Pd/Fe-C electrode. On all accounts, there was no significant variation in the removal efficiency of chloroacetic acids during dechlorination reaction under pH from 2 to 9, indicating that catalytic dechlorination of chloroacetic acids could be performed well under a wide pH range.

3.4. Effect of electrical bias potential on the removal efficiency of chloroacetic acids

Effect of electrical bias potential on the dechlorination of chloroacetic acid was also investigated. As shown in Fig. 5, the removal efficiency of chloroacetic acids was greatly increased under applied bias potential of −1.5 V (vs SCE). Li et al. reported that reductive dehalogenation of chloroacetic acids happened at potentials more cathodic than −1.0 V where molecular hydrogen would evolve [12]. Moreover, Pd(0) played important roles in chemisorption and decomposition of hydrogen into atomic H*, a highly activated intermediate hydrogen radical [17]. Combined with the pH analysis, it was beneficial for indirect reductions of chloroacetic acids when cathodic potentials more than −1.0 V. But when the potentials were lower than −1.5 V, intense and profuse hydrogen bubbles would influence the electron conduction at the electrode surface; even worse, this would induce electrode passivation. Thus the dechlorination efficiency of chloroacetic acids decreased at potentials of −2.5 V.

Furthermore, the effect of electrode potential on the reaction rate constants (k_{obs}) of chloroacetic acids could be deduced by Bulter–Volmer equation [15]:

$$k_{obs} = k_0 e^{-\overrightarrow{\alpha} F(E-E_{eq})/RT} \quad (1)$$

Thus, according to Eq. (1), the ratio of reaction rate constants at two electrode potentials, E_1 and E_2, was given by

$$\frac{k_{obs1}}{k_{obs2}} = e^{-\overrightarrow{\alpha} F(E_1-E_2)/RT} \quad (2)$$

where k_0 is the standard rate constant, F is the Faraday constant, R is the gas constant, T is the temperature, and $\overrightarrow{\alpha}$ is the transfer coefficients for the reduction. Li and Farrell reported that the minimum value of the transfer coefficient was close to 0.5 for a multistep [15]. As shown in Fig. 5 inset, decreasing the electrode potential resulted in increases in the reaction rate constants of chloroacetic acids. However, the increases in the reaction rate constants were less than expected based on the behavior predicted by Eq. (2). The small potential dependence of the reaction rate constants indicated that the rate-limiting step for the dechlorination of chloroacetic acids

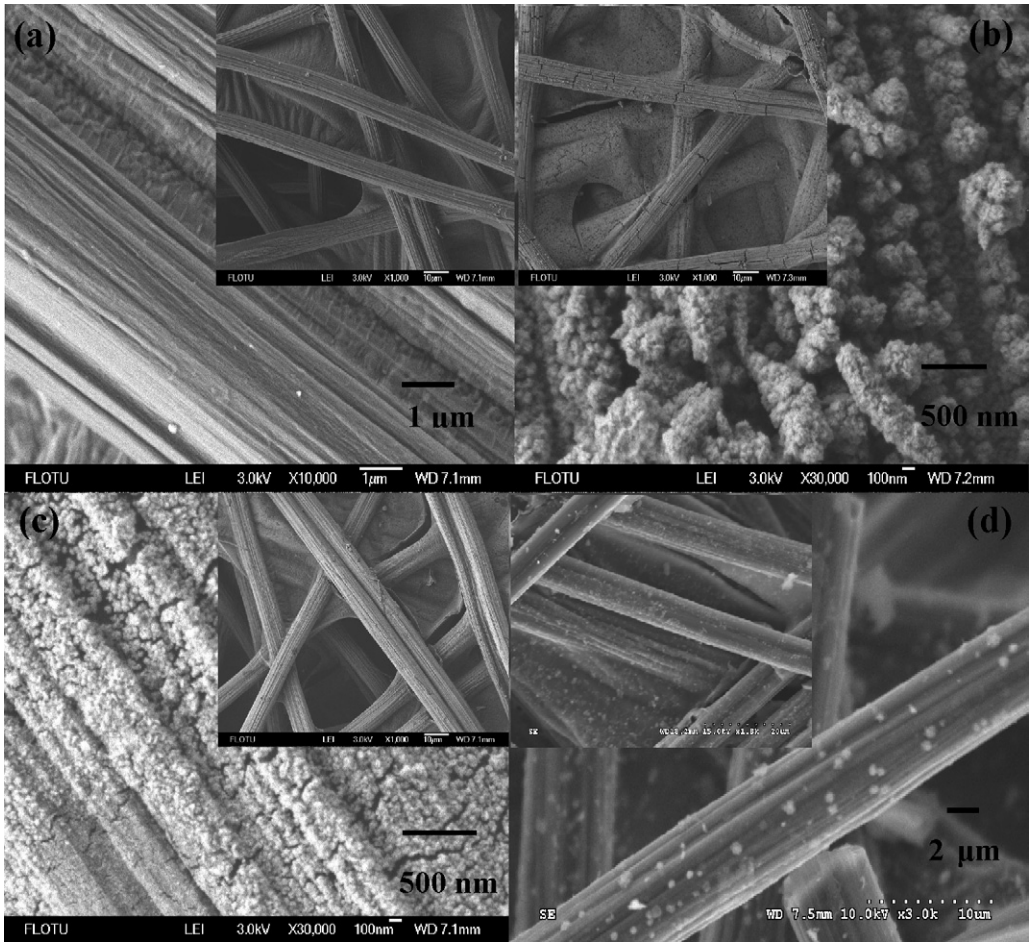

Fig. 6. SEM images of C, Pd-C and Pd/Fe-C electrodes. (a) C electrode; (b) electrodeposited Pd-C electrode; (c) electrodeposited Pd/Fe-C electrode; and (d) calcined Pd/Fe-C electrode.

did not only involve electron transfer. Thus, the primary dechlorination of chloroacetic acids was achieved by indirect reduction at Pd/Fe-C electrode.

3.5. Electrode characterization

The SEM images of C, Pd-C and Pd/Fe-C electrodes are given in Fig. 6(a), (b), (c) and (d), respectively. In comparison with Fig. 6(a) and (b), the electrodeposited Pd(0) particles were attached on the surface of carbon paper. The size of the Pd(0) particles was around 200 nm in diameter. As shown in Fig. 6(c) and (d), the diameters of electrodeposited and calcined Pd/Fe particles were around 20 nm and 400 nm, respectively. Additionally, the electrodeposited Pd/Fe particles were more compact than calcined Pd/Fe particles. The EDS patterns of Pd/Fe-C electrode exhibited the characteristic peaks of Pd and Fe, which are given in Supporting Information (Figure S6). It was concluded that Fe(0) particles were tightly attached between Pd(0) crystals under the influence of an electric field. The uniform dispersion and small size of the electrodeposited Pd/Fe particles on carbon paper were beneficial to the dechlorination reaction. The XRD patterns of C, Fe-C, Pd-C and Pd/Fe-C electrodes are presented in the Supporting Information (Figure S7). For both electrodeposited and calcined Pd/Fe-C electrodes, they showed metallic Pd and poorly metallic Fe peaks. Thus, this low concentration of Fe(0) was thought to be amorphous and existed in a highly dispersed state.

The valence state of Pd coated on Pd/Fe-C electrode was studied by XPS before and after the dechlorination of chloroacetic acids (Fig. 7). Due to the Pd $3p_{5/2}$ overlapped O 1s peak, the Pd 3d peak could be used to illustrate the valence state of Pd [33]. The binding energies (BE) of Pd 3d peaks at 335.3 eV and 340.6 eV showed the Pd(0) species before reaction. However, after the reaction, the presence of Pd(0) and Pd(II) species for the used Pd/Fe-C cathode indicated the formation of transitional C–Pd–Cl bond during dechlorination process. In the reaction process, the BE of Fe 2p

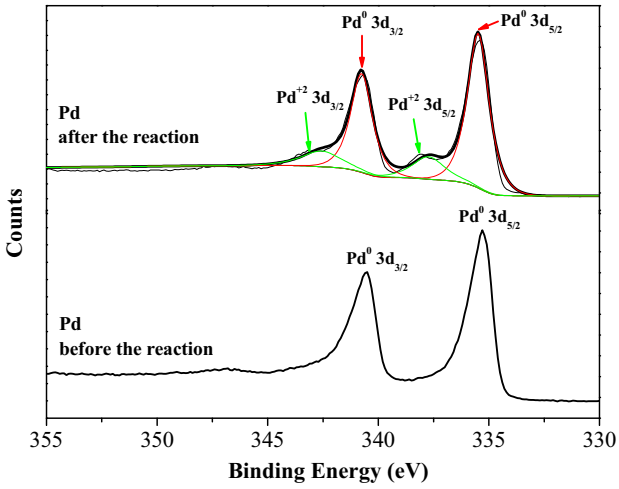

Fig. 7. XPS spectra of Pd on the Pd/Fe-C electrode before and after the dechlorination reaction.

photoelectron spectrum of the Pd/Fe-C electrode increased slightly (Figure S8), indicating the stability of Fe(0) species. Combined with the SEM analysis, increase of electrocatalytic activity by Fe(0) was due to the geometric effect.

3.6. Electrochemical analysis

To illustrate the electrochemical activity of the electrodes, the LSV and EIS display of C, Fe-C, Pd-C and Pd/Fe-C electrodes are presented in Fig. 8. The LSV measurement showed an increase in reduction current of Pd/Fe-C electrode in comparison to C, Pd-C and Fe-C electrodes (Fig. 8(a)). Moreover, with an increase of the initial DCAA concentration from 0 to 15 mg/L, an increase in cathodic current was clearly observable (Fig. 8(b)). The bimetallic Pd/Fe catalysts may enhance the transfer of electrons on the carbon paper through the external circuit to the cathode, thus producing additional cathodic current in contrast to a monometallic catalyst. In addition, there would be more electrons took part in the dechlorination process with increasing the initial concentration of chloroacetic acids on Pd/Fe-C electrode, then the interfacial reaction was intensified leading to an increase in cathodic current.

Fig. 8(c) illustrates that the arc curvature of the EIS Nyquist plot was intensified at electrodeposited Pd/Fe-C electrode, indicating that interfacial charges transferred to the electron acceptor taking place at electrodeposited Pd/Fe-C electrodes were faster than other electrodes. Combined with the SEM and LSV analysis, it could be deduced that electrodeposited Pd/Fe-C electrode exhibited higher electrocatalytic activity than calcined Pd/Fe-C electrode. Compared with the individual Pd-C electrode, in situ formation of Fe(0) decreased the interface impedance and accelerated the electron transfer at the electrode. That was in accordance with the results of chloroacetic acids dechlorination.

3.7. Proposed mechanism for electrocatalytic reduction of chloroacetic acids

It has been indicated that dechlorination intermediates and efficiency of chloroacetic acids at C, Fe-C, Pd-C, and Pd/Fe-C electrodes were different. On the basis of the experimental observations, it could be proposed that the dechlorination of chloroacetic acids proceeded by direct and indirect reduction, as depicted in Fig. 9. The direct reduction of TCAA was possibly stepwise, following the pathway (3)–(6):

$$Cl_3CCOOH + e^- \rightarrow Cl_2\dot{C}COOH + Cl^- \quad (3)$$

$$Cl_2\dot{C}COOH + H^+ + e^- \rightarrow Cl_2CHCOOH \quad (4)$$

$$Cl_2CHCOOH + e^- \rightarrow Cl\dot{C}HCOOH + Cl^- \quad (5)$$

$$Cl\dot{C}HCOOH + H^+ + e^- \rightarrow ClCH_2COOH \quad (6)$$

During the direct reduction process, TCAA first obtained an electron from the cathode to form a dichloroacetic radical. Then, the dichloroacetic radical received another electron from the cathode and through protonation lead to the formation of DCAA. Similar to the dechlorination process from TCAA to DCAA, MCAA was formed through two successive one-electron reductions steps of DCAA. MCAA cannot be dechlorinated during direct reduction process.

Based on the effect of initial pH and electrical bias potential on the dechlorination of chloroacetic acids, it could be deduced that presence of Pd(0) played a significant role in forming atomic H*. Combined with the SEM, XPS, LSV and EIS analysis, it was concluded that in situ formation of Fe(0) could modify the Pd(0) dispersion state, thus leaving the Pd component active and enhancing the transport of electrons at the cathode.

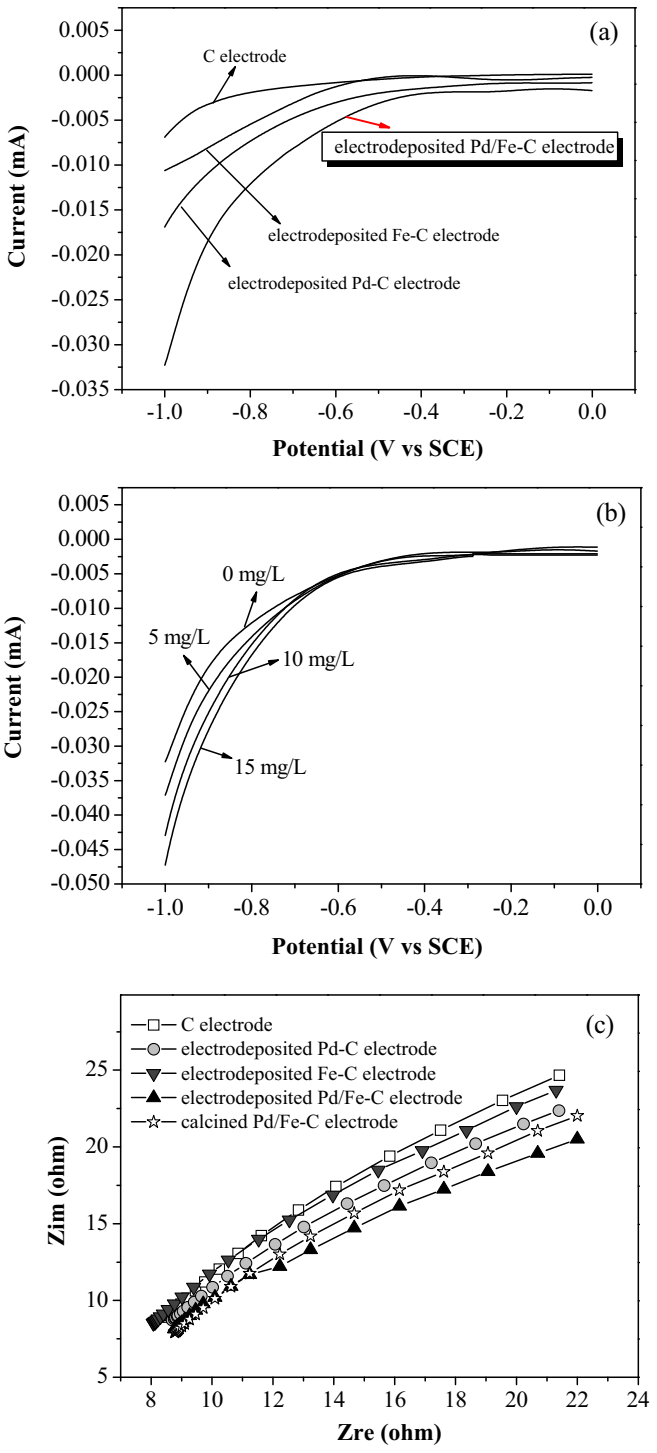

Fig. 8. LSV and EIS display of C, Pd-C, Fe-C and Pd/Fe-C electrodes. (a) LSV performance of the electrodes (initial concentration of DCAA: 5 mg/L); (b) LSV display of Pd/Fe-C electrode with gradient concentration of DCAA; and (c) EIS performance of the electrodes.

The indirect reduction of chloroacetic acids may follow the pathway (7)–(14):

$$H^+ + e^- \rightarrow H(Ads) \quad (7)$$

$$Pd + H(Ads) \rightarrow PdH* \quad (8)$$

$$Cl_3CCOOH + H* \rightarrow Cl_2CHCOOH + Cl^- \quad (9)$$

$$Cl_2CHCOOH + H* \rightarrow ClCH_2COOH + Cl^- \quad (10)$$

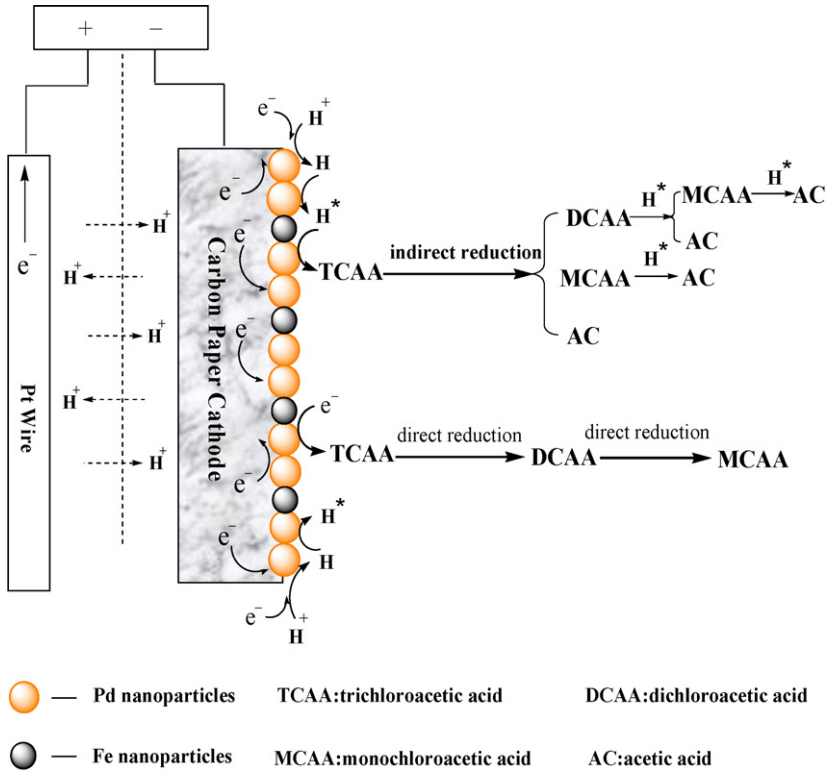

Fig. 9. Schematic illustration of the electrocatalytic dechlorination process by Pd/Fe-C cathode.

$$ClCH_2COOH + H* \rightarrow CH_3COOH + Cl^- \quad (11)$$

$$Cl_3CCOOH + 2H* \rightarrow ClCH_2COOH + 2Cl^- \quad (12)$$

$$ClCH_2COOH + 2H* \rightarrow CH_3COOH + 2Cl^- \quad (13)$$

$$Cl_3CCOOH + 3H* \rightarrow CH_3COOH + 3Cl^- \quad (14)$$

According to the above equations, it was indicated that the indirect reduction of chloroacetic acids might follow these routes: first, Pd(0) used the electron delivered from the cathode to transform H^+ into atomic H^*. Then the oxidative addition proceeded as forming a transitional C–Pd–Cl bond at the surface of Pd/Fe nanoparticles. The produced chloroacetic acids were then attacked with atomic H^*, followed by the C–Cl scission. Reduction of the Pd(II) at the cathode would regenerate active Pd(0) species, and the electrocatalytic cycle would continue. Moreover, the direct reduction was insignificant over distances greater than 10 Å (10^{-10} m) from the electrode surface [15]. Therefore, the indirect reduction which was achieved by atomic H^* could be the primary reaction to realize dechlorination of chloroacetic acids. After being used for 10 times, the removal efficiency of chloroacetic acids decreased 6%, which indicated the stability of Pd/Fe-C electrode.

4. Conclusions

In conclusion, Pd/Fe-C electrode prepared via electrodeposition showed higher activity in dechlorination of chloroacetic acids than via impregnation and calcination. The optimal molar ratio of Pd:Fe, the electrical bias potential and the initial pH value of reaction system for higher removal efficiency of chloroacetic acids at electrodeposited Pd/Fe-C electrodes were determined. SEM analysis of the electrodes revealed that the electrodeposited particles of Pd/Fe were smaller and more compact than calcined particles. The role of Pd(0) was to form atomic H^* which improved the dechlorination efficiency of chloroacetic acids. The presence of Fe(0) nanoparticles played a significant role in modifying the Pd(0) dispersion state.

Moreover, the dechlorination efficiency of chloroacetic acids followed the order of TCAA > DCAA > MCAA. Stepwise dechlorination of TCAA and DCAA to MCAA was observed via direct reduction. MCAA cannot be dechlorinated via direct reduction through electron transfer at the electrodes. However, a direct dechlorination pathway from chloroacetic acids to acetic acids was achieved via indirect reduction. Indirect reduction by atomic H^* was the primary process to realize the complete dechlorination of chloroacetic acids by Pd/Fe-C cathode.

Acknowledgments

This project is supported by Fund for the Creative Research groups of China (Grant 50921064) and the National Basic Research Program of China (Grant 2010CB933604). The kind suggestions from the editor and reviewers are deeply appreciated.

Appendix A. Supplementary data

Supplementary data associated with this article can be found, in the online version, at doi:10.1016/j.apcatb.2011.11.016.

References

[1] R.F. Christman, D.L. Norwood, D.S. Millington, J.D. Johnson, A.A. Stevens, Environ. Sci. Technol. 17 (1983) 625–628.
[2] C. Legay, M.J. Rodriguez, R. Sadiq, J.B. Serodes, P. Levallois, F. Proulx, J. Environ. Manage. 92 (2011) 892–901.
[3] I. Kristiana, C. Joll, A. Heitz, Chemosphere 83 (2011) 661–667.
[4] K. Gopal, S.S. Tripathy, J.L. Bersillon, S.P. Dubey, J. Hazard. Mater. 140 (2007) 1–6.
[5] B.M. McRae, T.M. LaPara, R.M. Hozalski, Chemosphere 55 (2004) 915–925.
[6] H.H. Tung, Y.F. Xie, Water Res. 43 (2009) 971–978.
[7] H. Czili, A. Horvath, Appl. Catal. B: Environ. 89 (2009) 342–348.
[8] D. Spangeberg, U. Moller, K. Kleinermanns, Chemosphere 33 (1996) 43–49.
[9] R.M. Hozalski, L. Zhang, W.A. Arnold, Environ. Sci. Technol. 35 (2001) 2258–2263.

[10] L. Zhang, W.A. Arnold, R.M. Hozalski, Environ. Sci. Technol. 38 (2004) 6881–6889.
[11] G.V. Korshin, M.D. Jensen, Electrochim. Acta 47 (2001) 747–751.
[12] Y.P. Li, H.B. Cao, Y. Zhang, Water Res. 41 (2007) 197–205.
[13] L. Altamar, L. Fernandez, C. Borras, J. Mostany, H. Carrero, B. Scharifker, Sens. Actuators B: Chem. 146 (2010) 103–110.
[14] N.S. Babu, N. Lingaiah, J.V. Kumar, P.S.S. Prasad, Appl. Catal. A: Gen. 367 (2009) 70–76.
[15] T. Li, J. Farrell, Environ. Sci. Technol. 34 (2000) 173–179.
[16] B.W. Zhu, T.T. Lim, Environ. Sci. Technol. 41 (2007) 7523–7529.
[17] X.Y. Wang, P. Ning, H.L. Liu, J. Ma, Appl. Catal. B: Environ. 94 (2010) 55–63.
[18] T.T. Dong, H. Luo, Y.P. Wang, B.J. Hu, H. Chen, Desalination 271 (2011) 11–19.
[19] A. Barrera, M. Viniegra, S. Fuentes, D. Gabriela, Appl. Catal. B: Environ. 56 (2005) 279–288.
[20] H.L. Lien, W.X. Zhang, Appl. Catal. B: Environ. 77 (2007) 110–116.
[21] Y.H. Shih, M.Y. Chen, Y.F. Su, Appl. Catal. B: Environ. 105 (2011) 24–29.
[22] N. Lingaiah, M.A. Uddin, A. Muto, Y. Sakata, Chem. Commun. (1999) 1657–1658.
[23] H. Choi, S. Agarwal, S.R. Alabed, Environ. Sci. Technol. 43 (2009) 488–493.
[24] C. Paoletti, A. Cemmi, L. Giorgi, R. Giorgi, L. Pilloni, E. Serra, M. Pasquali, J. Power Sources 183 (2008) 84–91.
[25] R. Rego, C. Oliveira, A. Velazquez, P.L. Cabot, Electrochem. Commun. 12 (2010) 745–748.
[26] Z.M. Pedro, E. Diaz, A.F. Mohedano, J.A. Casas, J.J. Rodriguez, Appl. Catal. B: Environ. 103 (2011) 128–135.
[27] K.D. Beard, J.W.V. Zee, J.R. Monnier, Appl. Catal. B: Environ. 88 (2009) 185–193.
[28] Y. Wang, J.H. Qu, Water Environ. Res. 78 (2006) 724–729.
[29] R. Muftikian, Q. Fernando, N. Korte, Water Res. 41 (1995) 2434–2439.
[30] T.L. Johanson, M.M. Scherer, P.G. Tratnyek, Environ. Sci. Technol. 30 (1996) 2634–2640.
[31] K. Mackenzie, H. Frenzel, F.D. Kopinke, Appl. Catal. B: Environ. 63 (2006) 161–167.
[32] E.V. Golubina, E.S. Lokteva, V.V. Lunin, N.S. Telegina, A.Y. Stakheev, P. Tundo, Appl. Catal. A: Gen. 302 (2006) 32–41.
[33] R. Muftikian, K. Nebesny, Q. Fernando, A.N. Korte, Environ. Sci. Technol. 30 (1996) 3593–3596.